Quantification of the chemical composition variations of tumors in photothermal therapy by photoacoustic spectroscopy: An in vitro study

Yubin Liu[a,b], Zhifang Li[b], Hui Li[b,*] and Zhen Yuan[a,*]

[a]*Bioimaging Core, Faculty of Health Sciences, University of Macau, Macau SAR, China*
[b]*College of Photonic and Electronic Engineering, Fujian Normal University, Fuzhou 350007, China*

Abstract. In this study, the change of tumors' chemical composition in the temperature range of 20 ~70ºC is quantified for photothermal tumor therapy by photoacoustic spectroscopy (PAS) with the wavelengths of 700~1000 nm. Based on the measured photoacoustic signals, two absorption peaks at the wavelengths of 750nm and 950nm are identified. It is also observed that high temperature (>55ºC) is able to induce the physical and chemical degeneration of tumors. According to the in vitro tests, a new chemical species, met-hemoglobin, which is absent in normal blood, is generated at high temperature with enhanced near-infrared absorption.

Keywords: PAS, photothermal therapy, photoacoustic signals, hemoglobin

1. Introduction

Photoacoustic spectroscopy (PAS) is a spectral approach that allows for direct measurements of tissue chromophores and other physiology parameters using multiple-wavelength laser illumination. PAS is based upon the photoacoustic effect, in which the laser-produced temperature rise and subsequent thermoelastic expansion of tissues generate acoustic waves which is detected by ultrasound transducers along multiple boundary positions. PAS was first used to measure the physical parameters of gas and now has become an essential tool to quantify tissue physiological functions, disease progression, responses to intervention and photothermal cancer therapy [1–6]. If we search the term "photoacoustic spectroscopy" using PubMed, we will find that the number of publications on PAS has increased from several in 1970 to almost a thousand to date.

In addition, photothermal therapy is a laser-based mini-invasive technique with extensive clinical and pre-clinical applications. It utilizes high continuous light intensity to irradiate the diseased tissues,

---

*Corresponding author: Hui Li, College of Photonic and Electronic Engineering, Fujian Normal University, Fuzhou 350007, China. Tel.: 059122868133; Fax: 059122868133; E-mail: hli@fjnu.edu.cn.
Zhen Yuan, Bioimaging Core, Faculty of Health Sciences, University of Macau, Macau SAR, China. Tel.: 85388224989; Fax: 85388222314; E-mail: zhenyuan@umac.mo.

which is able to convert light energy to heat, causing localized thermal destruction of tissues [7,8]. The definition of the critical temperature of hyperthermia, coagulation, vaporization, carbonization and fusion induced by laser has been proposed for in vivo study of photothermal cancer therapy [9]. Based on this, the temperature ranging from 42°C to 50°C is generally called hyperthermia, in which the tissues or organs will become necrotic if the laser irradiation lasts for a few minutes. And if temperature is over 60°C, the irradiation will lead to condensation of tissues and necrocytosis of cells as well as the denaturation of protein and collagen. This study will utilize PAS to measure and monitor the physiology parameters and chemical composition variations of tumors during photothermal therapy. Due to the use of multiple laser wavelengths, PAS is able to provide more accurate measurements of functional parameters including changes of hemoglobin and other species. Finally, in vitro tests will be used to demonstrate and validate PAS method for photothermal therapy.

2. Materials and methods

2.1. The theoretical foundation of PAS

Based on the photoacoustic effect, PAS uses a short pulse laser to illuminate the absorbers in tissues to generate the acoustic waves. The measured photoacoustic (PA) pressure that satisfies the temporal stress confinement is written as [1–5]:

$$P(z) = (\beta c^2 / C_p)\mu_a F(z) = (\beta c^2 / C_p)\mu_a F_0 \exp(-\mu_a z) \tag{1}$$

in which β is the expansion coefficient, c is the speed of sound, C_p is the specific heat, μ_a is the absorption coefficient of medium, F_0 is the initial optical fluence, and z is the one-dimensional incident depth at position z along the laser illumination direction. If the optical fluence F at different penetration depth is defined, the following equation will be obtained:

$$F = F_0 \exp(-\mu_a z) \tag{2}$$

Additionally, the light absorbed energy density is written as:

$$G = \mu_a F \tag{3}$$

It is noted from Eqs. (1)-(3) that the PA signal (pressure) is proportional to the light absorbed energy density G along the laser source incident direction: the maximum light energy is converted into thermal energy, i.e., the strongest PA signal. Here introduces a Grüneisen parameter Γ,

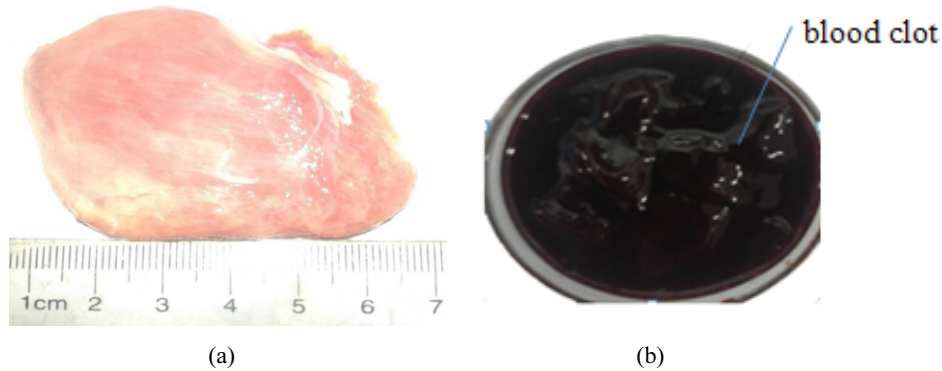$$\Gamma = \beta c^2 / C_p \tag{4}$$

Fig. 1. (a) The chicken breast and (b) the blood clot.

For soft tissues with temperature T between 10-55°C, the expansion coefficient β is linearly proportional to T [10,11],

$$\Gamma = A + BT \tag{5}$$

in which A and B are constants. As such, Eq. (1) can be further written as:

$$P(z) = \Gamma \mu_a F(z) = (A + BT(z))\mu_a F(z) = (A + BT(z))\mu_a F_0 \exp(-\mu_a z) \tag{6}$$

in which $T(z)$ is the temperature distribution of tissues. If the initial temperature distribution of tissues T_0 is assumed, Eq. (7) can be achieved:

$$P(z)_{T=T_0} = (A + BT_0)F_0 \exp(-\mu_a z) \tag{7}$$

In terms of Eqs. (6) and (7), the following Eq. (8) is obtained,

$$T(z) = (A + BT_0)P(z)\big/(BP(z)_{T=T_0}) - A/B = C + DP(z)\big/P(z)_{T=T_0} \tag{8}$$

in which $C=A/B$, $D=(A+BT_0)/B$ are parameters that are dependent on tissue properties, and $P(z)_{T=T_0}$ is the PA pressure profile recorded at the initial temperature. It is noted from Eq. (8) that the PA signal amplitudes is linearly proportion to the temperature. However, it only works well when the temperature is between 10-55°C. When the temperature is above 55°C, photochemical and photothermal modifications will exert an impact on the chemical constituents of blood, which will be validated by our new findings in Section 3. By querying data, we have found that a new chemical
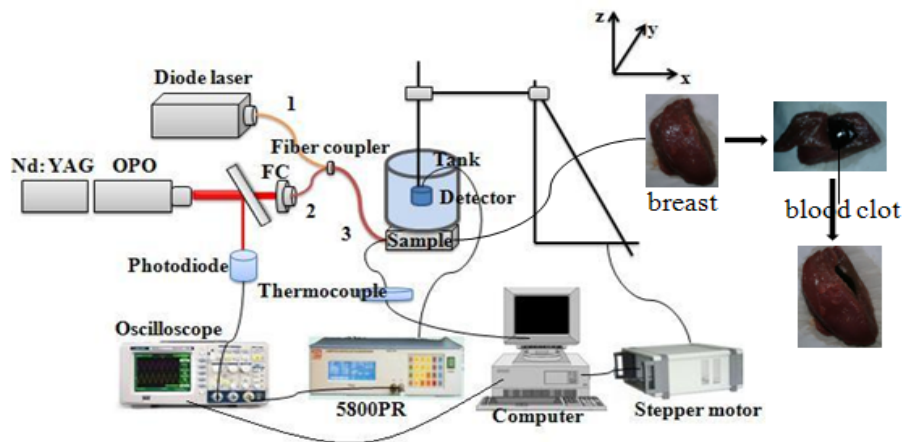
(a)
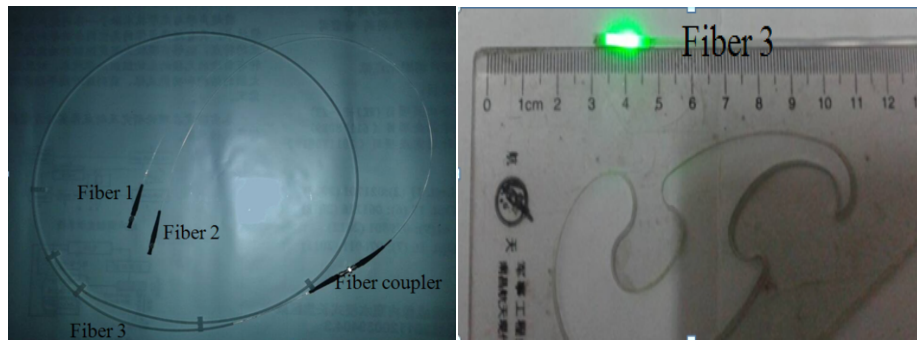
(b)   (c)

Fig. 2 (a) The experimental setup for exploring the physical and chemical mechanism of photothermal tumor therapy by PAS. (b) The diagram of two fiber coupling into a fiber by SMA interface. (c) The diagram of optical fiber dispersion.

species called met-hemoglobin is generated, which is closely related with the enhanced near-infrared absorption [12].

2.2. Materials

For the in vitro test, the blood clot as tumor simulation samples was buried inside the chicken breast, as plotted in Figure 1.

The experimental setup for PAS of photothermal tumor therapy is shown in Figure 2. The Nd: YAG laser (Surelite I-10, Continuum) with Optical Parametric Oscillator (OPO) (Surelite OPO plus, Continuum) was used for optoacoustic wave generation with a wavelength of 700~2000 nm, a repetition frequency rate of 10Hz, a pulse width of 5ns and the output energy of about 4 mJ. The diode laser treatment apparatus (ML-4030D) were used for photothermal tumor therapy, which could provide the power range of 1~30 W with the adjustable period of 0.5 W and the output wavelength of 810 nm. The fiber 1 was connected to the diode laser with the core diameter of 400 μm and maximum power threshold of 30 W. The fiber 2 was linked to the OPO laser by the FC interface, and the core

diameter of fiber 2 is 600 μm and the maximum power threshold is 6 W. The light beam from OPO is divided into two beams by splitter mirror: one is received by photodiode, displayed on the oscilloscope and then stored by a computer for calibration; the other one just focuses on the port of fiber 2 through a short focal length lens. Fiber 1 and fiber 2 were coupled by SMA interface formation of fiber 3, which had both the therapy and monitor functions, as displayed in Figures 2(b) and 2(c). The transmission wavelengths of optical fibers are between 500 and 2000nm. The dispersion end (length of 1.5 cm) of fiber 3 and the thermode (core diameter of 0.3 mm) were inserted into the tumor location of the sample. The upper surface of the sample was coupled with the soffit of the water bank by plastic wrap to reduce the sound attenuation between different media. The depth-resolved photoacoustic signals from the sample were collected by focused water immersion ultrasound transducer (Panametrics-NDT): the bandwidth of transducer ranges from 3.7 to 6.14 MHz, the center frequency is 5MHz and the water path is 25.654 mm, which means that the relative position of the probe with respect to the sample is about 25 mm. Then the signals were transferred to the ultrasonic receiver (5800 R, Parametric-NDT) for amplitude limit, filtering and amplifying. Finally, the signals were showed on the digital oscilloscope (TDS3054C, Tektronix). In order to improve the signal-to-noise ratio, the signals on the digital oscilloscope were taken averages of 16 times and then saved in the computer for the follow-up data processing. The stepper motor (SC300-2B, Zolix) could accurately control bracket by driving the electronic translation machine (TSA200-B, Zolix), for the 2D scanning of the sample.

3. Results

Figure 3 plots the near-infrared absorption spectra of the tumor simulation sample at various temperatures, in which x-axis represents different wavelengths while y-axis represents the photoacoustic signal amplitude with unit mV at different temperatures. It is observed from Figure 3 that there are two absorption peaks of blood: one is at 750 nm and the other is at 950 nm. This observation is in good agreement with the previous findings [13–15].

Figure 4 presents the relationship between the photoacoustic signals and temperatures at the wavelengths of 750 nm (Figure 4(a)) and 950 nm (Figure 4(b)) for two absorption peaks of blood in Figure 3. It is observed from Figure 4 that when the temperature is in the range of 20~55°C, a linear relationship exists between the photoacoustic signal amplitudes and the temperatures. However, this is not the case for the temperature over 55°C, where signals are increasing greater and quicker compared with those from 20~55°C. In addition, according to the previous findings [10], when temperature is over 60°C, the irradiation will lead to condensation of tissues and necrocytosis of cells as well as the denaturation of protein and collagen. These results and findings suggested that a new chemical species was produced and the linear relation between the signals and the temperature was no longer kept. By querying data, the new chemical species should be met-hemoglobin because the met- hemoglobin is implicated in the enhanced near-infrared absorption of blood [12–15]. And we believe the met-hemoglobin has larger absorption coefficient when the wavelength of pulsed laser source is larger than 600nm [16] In particular, several studies have demonstrated that in photothermal therapy the laser energy can alter the absorption characteristics of blood [17], in which the conversion of blood to a combination of met-hemoglobin and thrombus temporarily increases absorbance by approximately 3-5 times over that of normal blood [18,19]. Therefore, the mechanism and findings from previous work are in good agreement with ours.
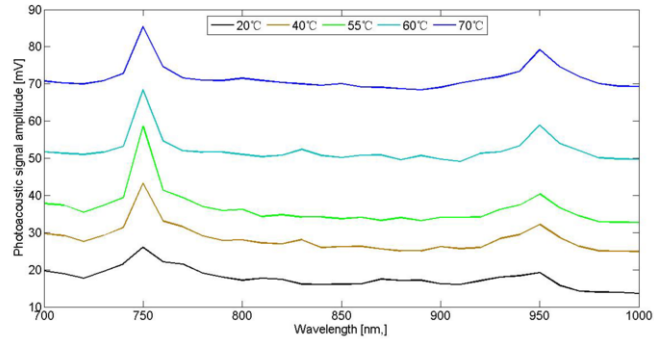
Fig. 3. The near-infrared absorption spectra of tumor simulation sample at various temperatures.
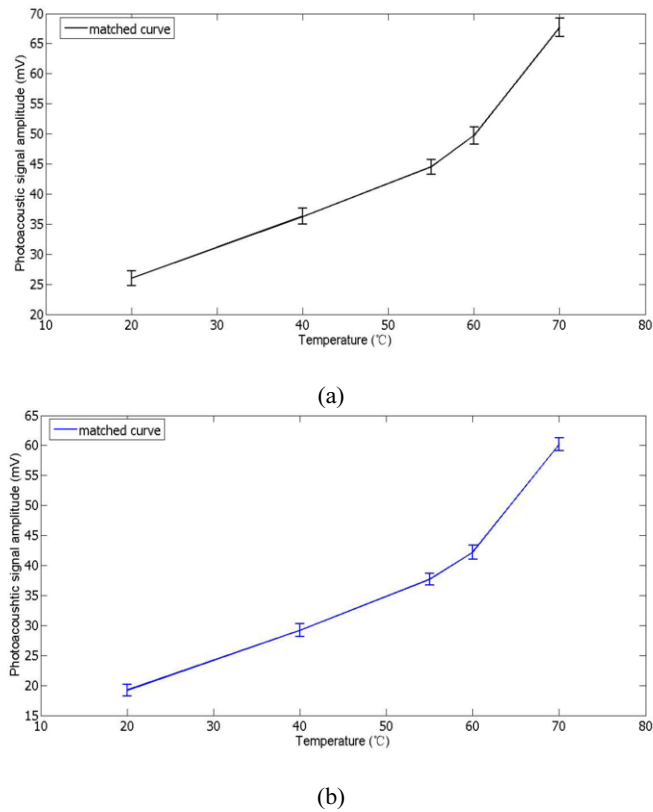

(a)

(b)

Fig. 4. (a) The relationship between photoacoustic signal amplitudes and temperatures at wavelengths 750 nm; (b) 950 nm.

Figures 5(a) and 5(b) displays the 2D scanning image of blood clot at wavelengths 750 nm and 950 nm, respectively, with temperature at 60°C, in which the x-axis is the sweep point (every bit of the step length is 0.1 mm and the total scanning length is 3 cm) while the y-axis represents the sampling numbers on the oscilloscope (every 1000 points are 2 μs). From Figure 5, the signals are in the range of point 50 to point 200, and the length of dispersion end of fiber 3 is 1.5 cm, which demonstrates that
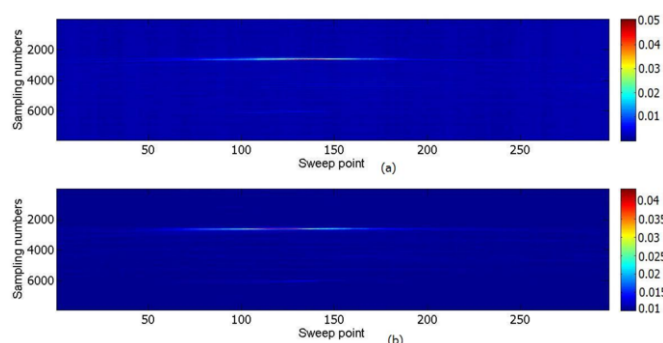
Fig. 5. (a) The 2D scanning image of blood clot with 750 nm at 60°C; (b) with 950 nm at 60°C.

the signals are from the excitation light source. Moreover, the strongest signals were generated by the blood clot. The grey values of image represent the information of photoacoustic signals and the values of color bar are equivalent to the amplitude of the photoacoustic signal. One can see from Figure 5 that the maximum amplitude of photoacoustic signal is 0.0497 V with the wavelength of 750 nm at 60°C, which also correlates well with the findings in Figure 3. If the relationship between the amplitude of photoacoustic signal and temperature is quantified, the grey-scale map of photoacoustic signal can be transformed into the image of temperature distribution.

4. Discussion

This study explored the photochemical degeneration of tumors during photothermal therapy by PAS. Two absorption peaks of blood were observed in vitro: one is 750 nm and the other is 950 nm. When the temperature is below 55°C, the two peaks occur due to the absorption of deoxy-hemoglobin, in which the photoacoustic signal amplitudes are proportional to the temperatures. However, when the temperature was over 55°C, a new chemical species was generated with the enhanced near-infrared absorption, destroying the linear relationship between the signals and the temperatures. In addition, 2D scanning images of the blood clot were also obtained at the wavelengths of 750 nm and 950 nm with temperature of 60°C.

A series of in vitro tests are conducted in this study to evaluate the performance of PAS systems. Though it works very well in terms of the quantitative findings, the controlled environments of in vitro tests are different from that of the non-controlled in vivo cases. As such, further investigations are required to extend the present study to *in vivo* pre-clinical small animal studies for cancer early detection and treatment. In addition, functional near infrared spectroscopy (fNIRS) can also quantify the physiological parameters of biological tissues [20–22]. However due to the low resolution of the diffuse light, the quantitative accuracy of PAS is much better than that from fNIRS, particularly for photothermal therapy related studies.

Additionally, our further investigation will be focused on quantifying the chromophore concentrations including oxy-hemoglobin concentration and deoxy-hemoglobin concentrations, and now efforts are spared to need incorporate the photon diffuse equation to separate the optical absorption coefficient from photon fluence [3].

Acknowledgment

References

[1]   A. Rosencwaig and J. Gersho, Theory of the photoacoustic effect with solids, J. Appl. Phys. **47** (1976), 64–69.

[2]   W.R. Harshbarger and M.B. Robin, The optoacoustic effect: revival of an old technique for molecular spectroscopy, Acc. Chem. Res. **6** (1973), 329–334.

[3]   Z. Yuan, X. Li and L. Xi, Listening to light scattering in turbid media: quantitative optical scattering imaging using photoacoustic measurements with one-wavelength illumination, J. Opt. **16** (2014), 065301–065309.

[4]   Christoph Haisch, Photoacoustic spectroscopy for analytical measurements, Meas. Sci. Technol. **23** (2012), 012001–012008.

[5]   P. Poulet, J. Chambron and R. Unterreiner, Quantitative photoacoustic spectroscopy applied to thermally thick samples, J. Appl. Phys. **51** (1980), 1738–1741.

[6]   Deepak V. Bageshwar, Avinash S. Pawar, Vineeta V. Khanvilkar and Vilasrao J. Kadam, Photoacoustic spectroscopy and its applications-A tutorial review, Eurasian J. Anal. Chem. **5** (2010), 187–203.

[7]   Jignesh Shah, Suhyun Park and Salavat Aglyamov et al., Photoacoustic imaging and temperature measurement for photothermal cancer therapy, Journal of Biomedical Optics **13** (2008), 034024.

[8]   K. Ivarsson, L. Myllymaki, K. Jabsner et al., Heat shock protein 70 (HSP70) after laser thermotherapy of an adenocarcinoma transplanted into rat liver, Anticancer Res. **23** (2003), 3703–3712.

[9]   Markolf H. Niemaz et al., Laser-Tissue Interactions: Fundamentals and Applications, Springer Science & Business Media, 2004.

[10] J. Shah, S. Park and S. Aglyamov et al., Photoacoustic imaging and temperature measurement for photothermal cancer therapy, J. Biomed. Opt. **13** (2008), 034024–034032.

[11] I.V. Larina, L.V. Larin and R.O. Esenaliev, Real-time optoacoustic monitoring of temperature in tissues, J. Phys. D: Appl. Phys. **38** (2005), 2633–2639.

[12] Jennifer Kehlet Barton, George Frangineas, Herbert Pummer and John F. Black, Cooperative phenomena in two-pulse, two-color laser photocoagulation of cutaneous blood vessel, Photochemistry and Photobiology **73** (2001), 642–650.

[13] Lorenzo Cordone, Antonio Cupane, Maurizio Leone and Eugenio Vitrano, Optical absorption spectra of deoxyhemoglobin and oxyhemoglobins in the temperature range 300-20 K relation with protein dynamics, Biophysical Chemistry **24** (1986), 259–275.

[14] William A. Eaton and James Hofrichter, Polarized absorption and linear dichroism spectroscopy of hemoglobin, Methods Enzymol. **76** (1981), 175–261.

[15] William A. Eaton , Louise Karle Hanson, P.J. Stephens, J.C. Sutherland and J.B.R. Dunn, Optical spectra of oxy- and deoxyhemoglobin, J. Am. Chem. Sot. **100** (1978), 4991–5003.

[16] O. Siggaard-Andersen, B. Norgaard-Pedersen and J. Rem, Hemoglobin pigments spectrophotometric determination of oxy-, carboxy-, met-, and sulfhemoglobin in capillary blood, Clinica. Chimica. Acta. **72** (1972), 85–100.

[17] J.F. Black and J.K. Barton, Time-Domain optical and thermal analysis of blood undergoing laser photocoagulation, Proc. of Laser-Tissue Interaction XII: Photochemical, Photothermal, and Photomechanical **4257** (2001), 341–354.

[18] J.T. Kuenstner and K.H. Norris, Spectrophotometry of human hemoglobin in the near infrared region from 1,000 nm to 2,500 nm, Journal of Near Infrared Spectroscopy **2** (1994), 59–65.

[19] M. Heger et al., Towards optimization of selective photothermolysis: prothromic pharmaceutical agents as potential adjuvants in laser treatment of port wine stains, Thromb. Haemost. **93** (2005), 242–256.

[20] Z. Yuan, A spatiotemporal and time frequency analysis of fNIRS brain signals using ICA method, Journal of Biomedical Optics **18** (2013), 106011–106018.

[21] Z. Yuan, Combing ICA and Granger causality to capture brain network dynamics with fNIRS measurements, Biomedical Optics Express **4** (2013), 2629–2643.

[22] Z. Yuan and J. Ye, Fusion of fNIRS and fMRI: Identification when and where hemodynamic responses are changing in human brain, Frontier in Human Neurosciences **7** (2013), 676–684.